Uptake and Release of Gaseous Species Accompanying the Reactions of Isoprene Photo-Oxidation Products with Sulfate Particles

Journal:	*Physical Chemistry Chemical Physics*
Manuscript ID	CP-ART-07-2015-004551.R1
Article Type:	Paper
Date Submitted by the Author:	17-Oct-2015

Complete List of Authors:	Liu, Yingjun; Harvard University, School of Engineering and Applied Sciences Kuwata, Mikinori; Harvard University, School of Engineering and Applied Sciences McKinney, Karena; Harvard University, School of Engineering and Applied Sciences Martin, Scot; Harvard University, School of Engineering and Applied Sciences; Harvard University, Department of Earth and Planetary Sciences

Uptake and Release of Gaseous Species Accompanying the Reactions of Isoprene Photo-Oxidation Products with Sulfate Particles

by

Yingjun Liu (1), Mikinori Kuwata[†] (1), Karena A. McKinney[*] (1), and Scot T. Martin[*] (1,2)

(1) School of Engineering and Applied Sciences, Harvard University, Cambridge, Massachusetts, USA

(2) Department of Earth and Planetary Sciences, Harvard University, Cambridge, Massachusetts, USA

E-mail: scot_martin@harvard.edu, kamckinney@seas.harvard.edu

Submitted: December 1, 2015

Physical Chemistry Chemical Physics

[*]To Whom Correspondence Should be Addressed

[†]Now at Asian School of the Environment, Nanyang Technological University, Singapore, and Earth Observatory of Singapore

Abstract

Gaseous species produced via the HO_2 reaction pathways of isoprene photo-oxidation were reacted with liquid, partially neutralized sulfate aerosol particles at 293 ± 1 K and <5% relative humidity. Isoprene-derived epoxydiols (IEPOX) were taken up for all neutralizations so long as the liquid phase was maintained. By comparison, isoprene-derived hydroperoxides (ISOPOOH) were taken up only for low neutralization (i.e., high acidity). The release of product molecules to the gas phase increased for low neutralization, corresponding to the release of at least 60 product molecules for the uptake of 100 reactant molecules at the lowest neutralization. A major reaction pathway was hydroperoxide cleavage in the particle phase to produce volatile products. Product species larger than the C_5 chain of isoprene were also released to the gas phase, implying that some accretion products in the particle phase were sufficiently volatile to partition to the gas phase. The study results show that the dependence of reactive uptake on neutralization varies by species. Furthermore, in addition to functionalization and accretion, decomposition and re-volatilization should be considered in mass balance formulations of reactive uptake by atmospheric particles.

1. Introduction

Secondary organic material (SOM) produced from the atmospheric oxidation of volatile organic compounds constitutes a large fraction of the mass concentration of atmospheric particles.[1] Negative bias in model predictions of SOM concentrations has been a topic of investigation.[2, 3] Underprediction might arise in part from chemical and physical processes not included in the models.[4, 5] The reactive uptake of gaseous species, particularly as catalyzed by the proton acidity of liquid sulfate particles, is considered one possible omitted process.[6-9] Organic species undergoing reactive uptake can include carbonyls,[10] hydroperoxides,[11] carboxylic acids,[12] epoxides,[13] and some hydrocarbons.[14-16] The reactions at least in part have an accretion characteristic, thereby leading to products of increased molecular weight and hence decreased volatility.[5, 8, 17]

Related mechanistic studies have largely focused on particle-phase products to infer the chemical mechanism. By comparison, changes of gaseous species in consequence to these reactions are less investigated. Surratt *et al.*[13] observed a significant decrease of gas-phase epoxides (IEPOX) upon mixing acidic sulfate particles with gas-phase products generated from isoprene oxidation. Iinuma *et al.*[18] reported the degassing of reaction products after the uptake of α- and β-pinene oxides to acidic sulfate particles. Herein, observations of the uptake and release of gaseous species are employed to study the mechanistic processes of the reactions of isoprene photo-oxidation products with sulfate aerosol particles. The first- and second-generation gas-phase oxidation products of isoprene via the OH/HO_2 reaction pathway are presented in Fig. 1.[19-22] The effect of the extent of sulfate neutralization on gas-particle exchange of these compounds and associated reactions is the focus of the present study.

2. Experimental

The experimental approach and collected data sets are described in Liu *et al.*[23] and Kuwata *et al.*[9] In brief, two continuously mixed flow reactors were connected in series and operated at steady state so as to separate the production of gaseous oxidation products of isoprene from the subsequent production of particulate SOM. In Reactor 1 (viz. the Harvard Environmental Chamber; HEC), isoprene photo-oxidation products were produced continuously. Photolysis of hydrogen peroxide was the OH source. The inflow and outflow isoprene concentrations were 120 ± 5 ppb and 36 ± 1 ppb, respectively. Reactor 1 had a mean residence time of 3.7 ± 0.3 h, a temperature of 293 ± 1 K, and a relative humidity of < 5%. The conditions were such that peroxy radicals $ROO^{\cdot}$, which were produced from OH/O_2 addition across the double bonds of isoprene, predominantly reacted with HO_2 rather than NO.[20] The outflow of Reactor 1 was mixed in Reactor 2 with either a flow of sulfate particles for reaction or zero air for reference. Reactor 2 had a mean residence time of 1.4 ± 0.1 h, a temperature of 293 ± 1 K, and a relative humidity of < 5%. Light was excluded from Reactor 2.

Sulfate particles were produced using two methods so as to achieve variable extents of neutralization.[9] Extent X of neutralization, defined as $n(NH_4^+)/(2n(SO_4^{2-}))$ for ion mole concentrations n(ion) (mol m^{-3}) of ions ammonium NH_4^+ and sulfate SO_4^{2-} in the particles, ranged from 0.0 for sulfuric acid to 1.0 for ammonium sulfate. Lower neutralization corresponds to higher acidity. In the first method, ammonium sulfate particles were exposed to sulfuric acid vapor to yield partially neutralized particles (i.e., $0.4 < X < 1.0$). The mass of the deposited vapor and hence the extent of neutralization were regulated by heating a reservoir of liquid sulfuric acid (96% w/w) to between 20 and 60 °C. In the second method, the vapor released from a reservoir of sulfuric acid at 67 °C was nucleated into new particles in the absence of ammonium

sulfate particles. Adventitious NH_3, however, somewhat neutralized the particles (X = 0.02). For X < 0.7, the sulfate particles were liquid, and significant SOM production was observed.[9]

Gaseous species in the outflow from Reactor 2 were sampled by a selective-reagent-ionization time-of-flight mass spectrometer (SRI-TOF-MS; NO^+ reagent; Ionicon Analytik GmbH).[24, 25] Exposure to sulfate particles (0.8 to 8.2 μg m^{-3}) led to changes in some gas-phase species concentrations in the outflow. Theses changes arose from the uptake or release of the gaseous species from the particles. Species concentrations came to steady state after 8 to 16 h.

A sensitivity factor was used to relate ion signal intensity after adjustment for ion transmission to species concentration in the gas phase. A factor of 22 ncps ppb^{-1} was used, as obtained by IEPOX calibration.[23] This quantification assumed that the reaction rate coefficient with NO^+ was the same as that of IEPOX for all other studied species. The uncertainty associated with this assumption led to an uncertainty of ± 50% (two-sigma) in measured species concentrations.[23] The unit "ncps" represents normalized counts per second, where the normalization was with respect to an NO^+ ion signal of 10^6 cps.

Particles in the outflow from Reactor 2 were sampled by a high-resolution time-of-flight Aerosol Mass Spectrometer (HR-TOF-AMS; Aerodyne Research Inc.).[26] Methods of data analysis were as described in Kuwata *et al.*[9] The extent of neutralization of the generated sulfate particles was determined from the ammonium and sulfate concentrations measured by the HR-TOF-AMS using constant relative ionization efficiencies.[27]

3. Results and Discussion

3.1 Families of reactants and products

Examples of unit-mass-resolution spectra obtained by sampling the outflow from Reactor 2 with the SRI-TOF-MS are shown in Fig. 2. The two spectra correspond to the absence

compared to the presence of sulfate particles (X = 0.02). The ratio I'/I of signal intensity at each m/z value of the two spectra is also plotted in Fig. 2. The notation used here shows quantities without prime as recorded in the absence of sulfate particles and quantities with prime as recorded in the presence of sulfate particles. The signal intensities for many m/z values decrease following the injection of liquid, partially neutralized sulfate particles (i.e., $I'/I < 1$). The signal changes arise from the loss of gaseous species to uptake by aerosol particles. There are also some signal intensities that do not change following particle injection (i.e., $I'/I = 1$ within uncertainty), such as those of $C_5H_8^+$ (m/z 68) from isoprene and $H_2O_2{\cdot}NO^+$ (m/z 64) from hydrogen peroxide. Finally, signal intensities at several m/z values increase following particle injection (i.e., $I'/I > 1$) (Fig. 2).

A ratio of $I'/I > 1$ indicates the release of a species from the particles, implying a sequence of events starting with the uptake of a gaseous reactant species, continuing by reactive transformation of this species inside the particle, and ending with the degassing of the product species. A control experiment using the SRI-TOF-MS to sample the particle flow upstream of Reactor 2, meaning before exposure to isoprene oxidation products, confirms that the ions characterized by $I'/I > 1$ are obtained only downstream of Reactor 2.

The high-mass-resolution counterpart of Fig. 2 shows that 43 carbonaceous ions have intensities above the background level (cf. Table S1). Each high-resolution ion is categorized into one of six characteristic families based on I'/I for intermediate ($0.4 < X < 0.7$) and low (X = 0.02) neutralization. Although no data are available for $0.02 < X < 0.4$ because of methods employed for particle generation (cf. Section 2), trends in I'/I in this range are not expected to alter the family designations. The complete set of ions for each family is listed in Table S1. The functional forms of $I'(X)$ and $I'/I\ (X)$ of one representative ion of each family are plotted in Figs.

3 and 4, respectively. Figure S1 presents additional examples of $I'(X)$ for more ions of individual families.

For ions of Family *N* ("null change for all studied neutralizations"; cf. Figs. 3 and 4), I'/I is unity within measurement uncertainty and does not vary with X. The conclusion is that no observable uptake occurs for species of Family *N*. For ions of Family L_{low} ("loss only for low neutralization"), I'/I is unity for intermediate neutralization but less than unity for particles of low neutralization (i.e., $X = 0.02$), meaning that the uptake of species of Family L_{low} is kinetically favorable only for low neutralization. For ions of Family *L* ("loss for both low and intermediate neutralizations"), I'/I progressively decreases from unity to below unity for decreasing neutralization. The ratio from X of 0.7 to 1.0 does not change, which is consistent with the observation of negligible production of SOM in the presence of solid sulfate particles (i.e., $X > 0.7$).[9] The uptake of species of Family *L* is therefore kinetically favorable across the full range of neutralization for which the sulfate particles are liquid. For ions of Family P_{low} ("production only for low neutralization"), I'/I is unity for intermediate neutralization but greater than unity for the low neutralization (i.e., $X = 0.02$). The release of gaseous species occurs only for the low neutralization. For ions of Family *P* ("production for both low and intermediate neutralizations"), I'/I progressively increases from unity to above unity with decreasing neutralization for $X < 0.7$ (i.e., liquid particles), meaning that reaction products are increasingly released to the gas phase. For ions of Family *LP* ("loss or production dependent on neutralization"), I'/I progressively decreases for particles of intermediate neutralization (i.e., $0.4 < X < 0.7$) followed by an increase at low neutralization (i.e., $X < 0.4$). The implication for Family *LP* is that uptake and release processes contribute to a net change in the observed ion signal, meaning that net uptake occurs for intermediate neutralization but release becomes important for low neutralization.

With respect to further analysis and discussion, the decrease of I to I' representing uptake is assumed to result exclusively from reactants in the case of Families L_{low} and L. Likewise, the increase of I to I' representing release is assumed to result exclusively from products in the case of Families P_{low} and P. Even so, a net process resulting in overall uptake or release, though not considered further herein, cannot be ruled out for these families. Family LP is taken to represent a group of species having net processes due to both reactants and products. With respect to quantitatively accounting for all species as well as tracking release and uptake of species of all the families during reactive uptake, Liu *et al*.[23] showed that the SRI-TOF-MS observations account for the carbon balance within uncertainty between the loss of isoprene and the appearance of oxidation products, at least for the studied experimental conditions.

Based on the foregoing observations, for intermediate neutralization Families L, P, and LP encompass the species undergoing uptake and release. Figure 5a shows the signal changes ΔI of species in these families. The summed signal changes for each of Families L, P, and LP are -116 ± 4 ncps, +27 ± 4 ncps, and -13 ± 2 ncps, respectively (cf. Table S2). The implication is that the uptake of 100 reactant molecules to the particle phase leads after reaction to the release of an upper limit of 30 molecules to the gas phase (95% confidence interval; cf. Table S3).

By comparison, for low neutralization the kinetically favorable processes expand and encompass the full range of species represented by Families L_{low}, L, P_{low}, P, and LP. Figures 5b and 5c show the signal changes ΔI. The summed changes for each of the five Families are -130 ± 7 ncps, -207 ± 4 ncps, +125 ± 5 ncps, +179 ± 6 ncps, and -2 ± 2 ncps, respectively (cf. Table S2). In this case, the uptake of 100 molecules to the particle phase after reaction leads to the release of a lower limit of 60 molecules. The implication is that the molecular yield of volatile products is greater for low compared to intermediate neutralization, suggesting that decomposition in

addition to functionalization and accretion becomes progressively more favorable for low neutralization.

3.2 Epoxides

For intermediate neutralization, the IEPOX pathway of isoprene oxidation is estimated to contribute half of the mass of isoprene-derived SOM.[23] The $C_5H_6O^+$ ion is the dominant ion produced by β-IEPOX isomers sampled by the SRI-TOF-MS, and this ion dominates the response of Family *L* for both low and intermediate neutralization (Figs. 5a and 5b). Major particle-phase reaction products of IEPOX isomers include methyl-butanetetrols, C_5-alkene triols, organosulfates, and various oligomers.[13] These products have low vapor pressures as well as high water solubility and thus remain in the particle phase, contributing substantially to SOM production.

Lower limits can be obtained of the neutralization-dependent reactive uptake coefficient γ_{IEPOX}. The lower limit for initial uptake ranges from 0.08 for intermediate neutralization to 0.20 for low neutralization (cf. Supplementary Material; Fig. S2a). For comparison, Gaston *et al*.[28] report $\gamma_{\mathrm{IEPOX}} = 0.10 \pm 0.01$ for $X = 0.5$ and 30% RH. The results of the two studies are in agreement within the uncertainties.

3.3 Hydroperoxides

Among ions of Family L_{low}, the signals for $C_4H_6NO_2^+$ and $C_4H_5O^+$ have the largest decreases, accounting for 81 ± 3 % of the total decrease of the family (Fig. 5c). These two ions originate mainly from isoprene-derived hydroperoxides (ISOPOOH). Methyl vinyl ketone (MVK) and methacrolein (MACR) make a significant but minor contribution of <20% to the intensities of these ions under the experimental conditions.[20] The ISOPOOH species are taken up

only for low neutralization (X = 0.02) (Fig. 5c). Surratt *et al.* [2010] also reported insignificant uptake of ISOPOOH for intermediate neutralization.

Section 3.1 concluded that decomposition is a favorable reaction pathway at low neutralization. Given that ISOPOOHs are the dominant species of Family L_{low}, the implication is that ISOPOOH species should follow decomposition pathways, at least in part. The decomposition of organic hydroperoxides at low neutralization originates by acid cleavage of the oxygen-oxygen bond, followed by 1,2-akyl shift of the resultant RO^+.[29-31] Among ISOPOOH isomers of isoprene oxidation (cf. Fig. 1), ISOPBOOH is the most important because it is at once the most abundant and the most reactive.[22] Reactivity decreases stepwise in the series of tertiary (ISOPBOOH), secondary (ISOPDOOH), and primary (ISOPAOOH and ISOPCOOH) hydroperoxides because the progressive substitution of the α-carbon makes the O-O bond more vulnerable to electrophilic attack.[29]

Major expected products from the acid cleavage of ISOPBOOH include hydroxyacetone ($C_3H_6O_2$) and acetaldehyde (C_2H_4O), as follows:

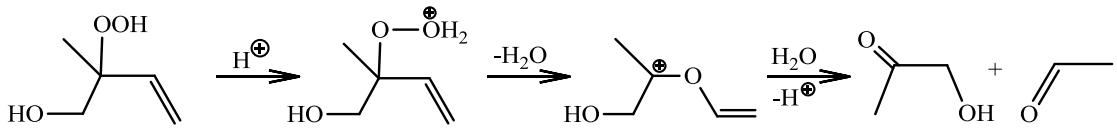

(1)

Standard addition shows that hydroxyacetone reacts with NO^+ to dominantly produce the $C_3H_6NO_3^+$ ion in the SRI-TOF-MS. The experimental results of Fig. 5c show that the $C_3H_6NO_3^+$ ion accounts for 83 ± 2 % of the total increase across all ions of Family P_{low} upon exposure to particles of low neutralization. The increase occurs only for low neutralization. The decrease in signal intensity for the $C_4H_6NO_2^+$ and $C_4H_5O^+$ ions of the ISOPOOH reactants in Family L_{low} is approximately equal to the increase in the signal intensity for the $C_3H_6NO_3^+$ ion of the hydroxyacetone product in Family P_{low}. Given the uncertainty of ± 50% in concentrations

estimated from signal intensities, the molecular ratio of hydroxyacetone release to ISOPOOH uptake has a lower limit of 0.5 (95% confidence interval).

The signal intensity of the major ion ($C_2H_3O^+$) of the other product acetaldehyde also increases for low neutralization, although to a lesser extent than for the $C_3H_6NO_3^+$ ion (Fig. S2b). The $C_2H_3O^+$ ion belongs to Family *LP* and is affected by both uptake and release processes. In addition to acetaldehyde, the $C_2H_3O^+$ ion can arise from larger compounds that fragment upon reaction with NO^+.[32]

3.4 Other reactants and products

Hydroxyl aldehydic epoxides ($C_5H_8O_3$; Fig. 1) have been proposed as C_5 gas-phase OH-oxidation products of IEPOX compounds.[21, 33] In this light, reactions of $C_5H_8O_3$ epoxides with NO^+ could give rise to an $C_5H_7O_2^+$ ion by abstraction of a hydroxide ion (i.e., $C_5H_8O_3$ - OH^-), which is a common reaction pathway with NO^+ for compounds having a hydroxyl group.[34] The $C_5H_7O_2^+$ ion is observed as second largest contributor to Family *L* (Figs. 5a and 5b) for both low and intermediate neutralization.

For Family *P*, $C_5H_8NO_4^+$ is the major ion (Figs. 5a and 5b). It can be regarded as a cluster ion of $C_5H_8O_3$ with the NO^+ reagent ion. Its precursor molecule is produced in the particle phase and then released to the gas phase. The molecule might be produced by the acid-catalyzed isomerization of isoprene photo-oxidation products. The transformation of epoxides[35] or 1,4-hydroxylcarbonyls[36] by this mechanism to produce hydrofurans is one possibility. Hydrofurans of $C_5H_8O_3$ are sufficiently volatile for release to the gas phase[37] and are expected to cluster with NO^+ in SRI-TOF-MS.

There is evidence for particle-phase reactions that link smaller chain reactants together and release longer-chain volatile products to the gas phase. In the absence of particle exposure,

there are no ions larger than C_5 detected by the SRI-TOF-MS. This result is expected given that isoprene is a C_5 compound and that photo-oxidation reactions typically do not increase carbon chain length. By comparison, after particle exposure highly oxygenated C_6-C_7 ions, such as $C_6H_8NO_5^+$, $C_7H_{12}NO_5^+$, $C_6H_{10}NO_5^+$, and $C_6H_8NO_6^+$, contribute to Family P_{low} (Fig. 5c). The detection of ions larger than C_5^+ implies that accretion reactions take place in the particle phase and that some of these products are sufficiently volatile to partition to the gas phase. Associated reaction mechanisms can include peroxyhemiacetal and peroxyacetal pathways of hydroperoxides in reaction with aldehydes.[11, 38]

4. Conclusions

Of 43 analyzed ions, six ions account for 66 ± 4 % of the total decrease and 61 ± 14 % of the total increase in signal intensities for low neutralization. For intermediate neutralization, the respective quantities are 71 ± 2 % and 76 ± 2 %. The four major ions contributing to signal decrease (i.e., uptake) include $C_5H_6O^+$ as IEPOX, $C_4H_6NO_2^+$ and $C_4H_5O^+$ as ISOPOOH, and $C_5H_7O_2^+$ possibly as hydroxyl aldehydic epoxides. The two major ions associated with signal increase (i.e., release) include $C_3H_6NO_3^+$ as hydroxyacetone and $C_5H_8NO_4^+$ from undetermined compounds, possibly hydrofurans.

The results show that at least 50% of the ISOPOOH molecules taken up into the particle phase react to lead to volatile products that evaporate to the gas phase. The implication is that the contribution of ISOPOOH isomers to SOM production might be small, even for low neutralization. The degassing products could, however, undergo further photo-oxidation and contribute to further-generation SOM production.[18] By comparison, IEPOX uptake appears to lead to less-volatile products that remain in the particle phase and contribute to SOM production. The results presented herein call attention to the idea that not just functionalization and accretion

but also decomposition, isomerization, and re-volatilization should be considered when formulating the mass balance of reactive uptake processes of atmospheric particles.

Acknowledgments. Support was received from the U.S. National Science Foundation (Grant No. ATM-0959452) and the U.S. Department of Energy (Grant No. DE-FG02-08ER64529). Y.J. Liu acknowledges a NASA Earth and Space Science Fellowship. We acknowledge Dr. Y. Liu for assistance with instrument calibrations.

References

1. Q. Zhang, J. L. Jimenez, M. R. Canagaratna, J. D. Allan, H. Coe, I. Ulbrich, M. R. Alfarra, A. Takami, A. M. Middlebrook, Y. L. Sun, K. Dzepina, E. Dunlea, K. Docherty, P. F. DeCarlo, D. Salcedo, T. Onasch, J. T. Jayne, T. Miyoshi, A. Shimono, S. Hatakeyama, N. Takegawa, Y. Kondo, J. Schneider, F. Drewnick, S. Borrmann, S. Weimer, K. Demerjian, P. Williams, K. Bower, R. Bahreini, L. Cottrell, R. J. Griffin, J. Rautiainen, J. Y. Sun, Y. M. Zhang and D. R. Worsnop, *Geophys. Res. Lett.*, 2007, **34**, L13801.
2. C. L. Heald, D. J. Jacob, R. J. Park, L. M. Russell, B. J. Huebert, J. H. Seinfeld, H. Liao and R. J. Weber, *Geophys. Res. Lett.*, 2005, **32**, L18809.
3. A. H. Goldstein and I. E. Galbally, *Environ. Sci. Technol.*, 2007, **41**, 1514-1521.
4. A. G. Carlton, C. Wiedinmyer and J. H. Kroll, *Atmos. Chem. Phys.*, 2009, **9**, 4987-5005.
5. M. Hallquist, J. C. Wenger, U. Baltensperger, Y. Rudich, D. Simpson, M. Claeys, J. Dommen, N. M. Donahue, C. George, A. H. Goldstein, J. F. Hamilton, H. Herrmann, T. Hoffmann, Y. Iinuma, M. Jang, M. E. Jenkin, J. L. Jimenez, A. Kiendler-Scharr, W. Maenhaut, G. McFiggans, T. F. Mentel, A. Monod, A. S. H. Prevot, J. H. Seinfeld, J. D. Surratt, R. Szmigielski and J. Wildt, *Atmos. Chem. Phys.*, 2009, **9**, 5155-5236.
6. J. D. Surratt, M. Lewandowski, J. H. Offenberg, M. Jaoui, T. E. Kleindienst, E. O. Edney and J. H. Seinfeld, *Environ. Sci. Technol.*, 2007, **41**, 5363-5369.
7. M. Jang, N. M. Czoschke, S. Lee and R. M. Kamens, *Science*, 2002, **298**, 814-817.
8. P. J. Ziemann and R. Atkinson, *Chem. Soc. Rev.*, 2012, **41**, 6582-6605.
9. M. Kuwata, Y. Liu, K. McKinney and S. T. Martin, *Phys. Chem. Chem. Phys.*, 2015, **17**, 5670-5678.
10. M. Jang and R. M. Kamens, *Environ. Sci. Technol.*, 2001, **35**, 4758-4766.
11. K. S. Docherty, W. Wu, Y. B. Lim and P. J. Ziemann, *Environ. Sci. Technol.*, 2005, **39**, 4049-4059.
12. J. F. Hamilton, A. C. Lewis, J. C. Reynolds, L. J. Carpenter and A. Lubben, *Atmos. Chem. Phys.*, 2006, **6**, 4973-4984.

13. J. D. Surratt, A. W. H. Chan, N. C. Eddingsaas, M. N. Chan, C. L. Loza, A. J. Kwan, S. P. Hersey, R. C. Flagan, P. O. Wennberg and J. H. Seinfeld, *P. Natl. Acad. Sci. USA*, 2010, **107**, 6640-6645.
14. J. Liggio, S.-M. Li, J. R. Brook and C. Mihele, *Geophys. Res. Lett.*, 2007, **34**, L05814.
15. S. Enami, H. Mishra, M. R. Hoffmann and A. J. Colussi, *J. Phys. Chem. A*, 2012, **116**, 6027-6032.
16. S. Enami, M. R. Hoffmann and A. J. Colussi, *J. Phys. Chem. Lett.*, 2012, **3**, 3102-3108.
17. J. H. Kroll and J. H. Seinfeld, *Atmos. Environ.*, 2008, **42**, 3593-3624.
18. Y. Iinuma, A. Kahnt, A. Mutzel, O. Böge and H. Herrmann, *Environ. Sci. Technol.*, 2013, **47**, 3639-3647.
19. Y. J. Liu, M. Kuwata, B. F. Strick, F. M. Geiger, R. J. Thomson, K. A. McKinney and S. T. Martin, *Environ. Sci. Technol.*, 2015, **49**, 250-258.
20. Y. J. Liu, I. Herdlinger-Blatt, K. A. McKinney and S. T. Martin, *Atmos. Chem. Phys.*, 2013, **13**, 5715-5730.
21. A. Jordan, S. Haidacher, G. Hanel, E. Hartungen, L. Märk, H. Seehauser, R. Schottkowsky, P. Sulzer and T. D. Märk, *Int. J. Mass. Spectrom.*, 2009, **286**, 122-128.
22. A. Jordan, S. Haidacher, G. Hanel, E. Hartungen, J. Herbig, L. Märk, R. Schottkowsky, H. Seehauser, P. Sulzer and T. D. Märk, *Int. J. Mass. Spectrom.*, 2009, **286**, 32-38.
23. P. F. DeCarlo, J. R. Kimmel, A. Trimborn, M. J. Northway, J. T. Jayne, A. C. Aiken, M. Gonin, K. Fuhrer, T. Horvath, K. S. Docherty, D. R. Worsnop and J. L. Jimenez, *Anal. Chem.*, 2006, **78**, 8281-8289.
24. M. R. Canagaratna, J. T. Jayne, J. L. Jimenez, J. D. Allan, M. R. Alfarra, Q. Zhang, T. B. Onasch, F. Drewnick, H. Coe, A. Middlebrook, A. Delia, L. R. Williams, A. M. Trimborn, M. J. Northway, P. F. DeCarlo, C. E. Kolb, P. Davidovits and D. R. Worsnop, *Mass. Spectrom. Rev.*, 2007, **26**, 185-222.
25. C. J. Gaston, T. P. Riedel, Z. Zhang, A. Gold, J. D. Surratt and J. A. Thornton, *Environ. Sci. Technol.*, 2014, **48**, 11178-11186.
26. N. C. Deno, W. E. Billups, K. E. Kramer and R. R. Lastomirsky, *J. Org. Chem.*, 1970, **35**, 3080-3082.
27. J. O. Turner, *Tetrahedron Lett.*, 1971, **12**, 887-890.
28. R. D. Bushick, *Tetrahedron Lett.*, 1971, **12**, 579-582.
29. M. E. Jenkin, J. C. Young and A. R. Rickard, *Atmos. Chem. Phys. Discuss.*, 2015, **15**, 9709-9766.
30. P. Mochalski, K. Unterkofler, P. Španěl, D. Smith and A. Amann, *Rapid. Commun. Mass. Sp.*, 2014, **28**, 1683-1690.
31. K. H. Bates, J. D. Crounse, J. M. St. Clair, N. B. Bennett, T. B. Nguyen, J. H. Seinfeld, B. M. Stoltz and P. O. Wennberg, *J. Phys. Chem. A*, 2014, **118**, 1237-1246.
32. M. I. Jacobs, A. I. Darer and M. J. Elrod, *Environ. Sci. Technol.*, 2013, **47**, 12868-12876.
33. D. Smith and P. Spanel, *Mass. Spectrom. Rev.*, 2005, **24**, 661-700.
34. Y. H. Lin, Z. Zhang, K. S. Docherty, H. Zhang, S. H. Budisulistiorini, C. L. Rubitschun, S. L. Shaw, E. M. Knipping, E. S. Edgerton, T. E. Kleindienst, A. Gold and J. D. Surratt, *Environ. Sci. Technol.*, 2011, **46**, 250-258.
35. Y. B. Lim and P. J. Ziemann, *Phys. Chem. Chem. Phys.*, 2009, **11**, 8029-8039.
36. J. F. Pankow and W. E. Asher, *Atmos. Chem. Phys.*, 2008, **8**, 2773-2796.

37. J. D. Surratt, S. M. Murphy, J. H. Kroll, N. L. Ng, L. Hildebrandt, A. Sorooshian, R. Szmigielski, R. Vermeylen, W. Maenhaut, M. Claeys, R. C. Flagan and J. H. Seinfeld, *J. Phys. Chem. A*, 2006, **110**, 9665-9690.

List of Figures

Figure 1. Mechanism of isoprene oxidation via the HO_2 pathway to produce ISOPOOH isomers as major first-generation products and IEPOX isomers as major second-generation products. Abbreviations: ISOP (isoprene); ISOPOOH (isoprene hydroxyl hydroperoxide, $C_5H_{10}O_3$); MACR (methacrolein, C_4H_6O); MVK (methyl vinyl ketone, C_4H_6O); IEPOX (isoprene-derived hydroxyl epoxdies, $C_5H_{10}O_3$).

Figure 2. Unit-mass-resolution spectra collected by SRI-NO^+-TOF-MS of the outflow of Reactor 2 in the absence (I; purple) and the presence (I'; orange) of liquid, partially neutralized sulfate aerosol particles (X = 0.02). Also shown in gray is the ratio of the two spectra (I'/I). The red solid line represents a ratio of unity. The dashed red lines represent confidence intervals of 99.7% based on measurement uncertainty. Gray bars outside of the confidence intervals represent values of I'/I that are statistically significant different from unity.

Figure 3. Dependence of signal intensity I' on the extent X of neutralization in presence of particles for ions representative of the six general families of behavior: (N) $C_5H_8^+$, m/z 68.062; (L_{low}) $C_4H_6NO_2^+$, m/z 100.039; (L) $C_5H_6O^+$, m/z 82.041; (P_{low}) $C_3H_6NO_3^+$, m/z 104.034; (P) $C_5H_8NO_4^+$, m/z 146.045;, and (LP) $C_5H_9O_3^+$, m/z 117.055. The shaded areas represent confidential intervals of 99.7% of signal intensity I in the absence of sulfate particles. For many values of X, the signal intensity does not change in the presence of particles (i.e., data points overlying the shaded areas). The dotted lines represent a threshold of X = 0.7, which is the transition point of the sulfate particles from aqueous to solid for the conducted experiments.

Figure 4. Dependence on the extent X of neutralization of the ratio I'/I of signal intensity in presence compared to the absence of particles for ions representative of the six general families of behavior (cf. caption to Fig. 3). For many values of X, the signal intensity does not change in the presence of particles (i.e., the ratios are close to unity). The dotted lines represent a threshold of $X = 0.7$, which is the transition point of the sulfate particles from aqueous to solid for the conducted experiments.

Figure 5. Change ΔI in signal intensity after the introduction of sulfate particles (i.e., $\Delta I = I' - I$). (a) Families L, P, and LP for intermediate neutralization. (b) Families L, P, and LP for low neutralization. (c) Families L_{low} and P_{low} for low neutralization.

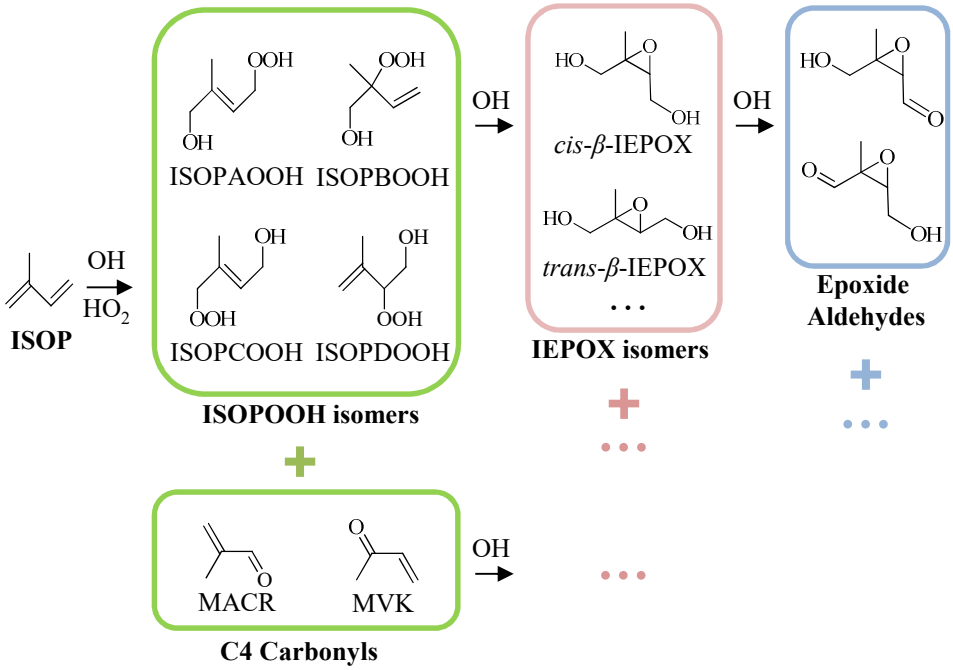
ISOP
OH
HO2
OOH
OH
ISOPAOOH
ISOPBOOH
ISOPCOOH
ISOPDOOH
ISOPOOH isomers
MACR
MVK
C4 Carbonyls
HO
O
cis-β-IEPOX
trans-β-IEPOX
IEPOX isomers
Epoxide
Aldehydes

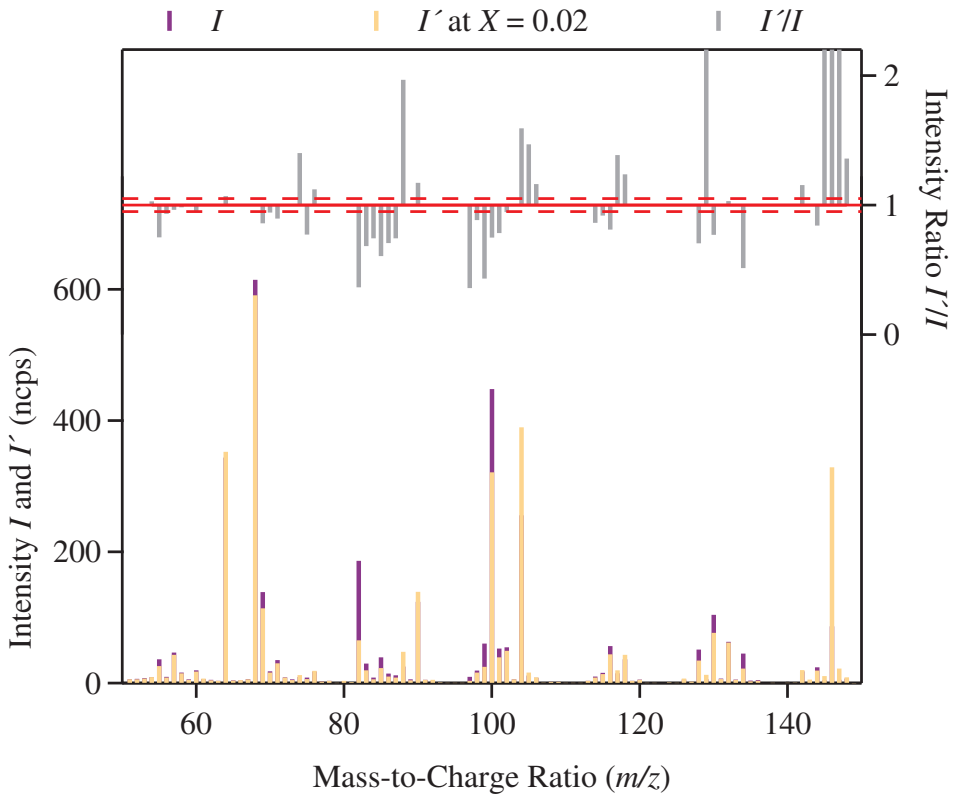
I
I´ at X = 0.02
I´/I
Intensity Ratio I´/I
2
1
0
600
400
200
0
Intensity I and I´ (ncps)
60
80
100
120
140
Mass-to-Charge Ratio (m/z)

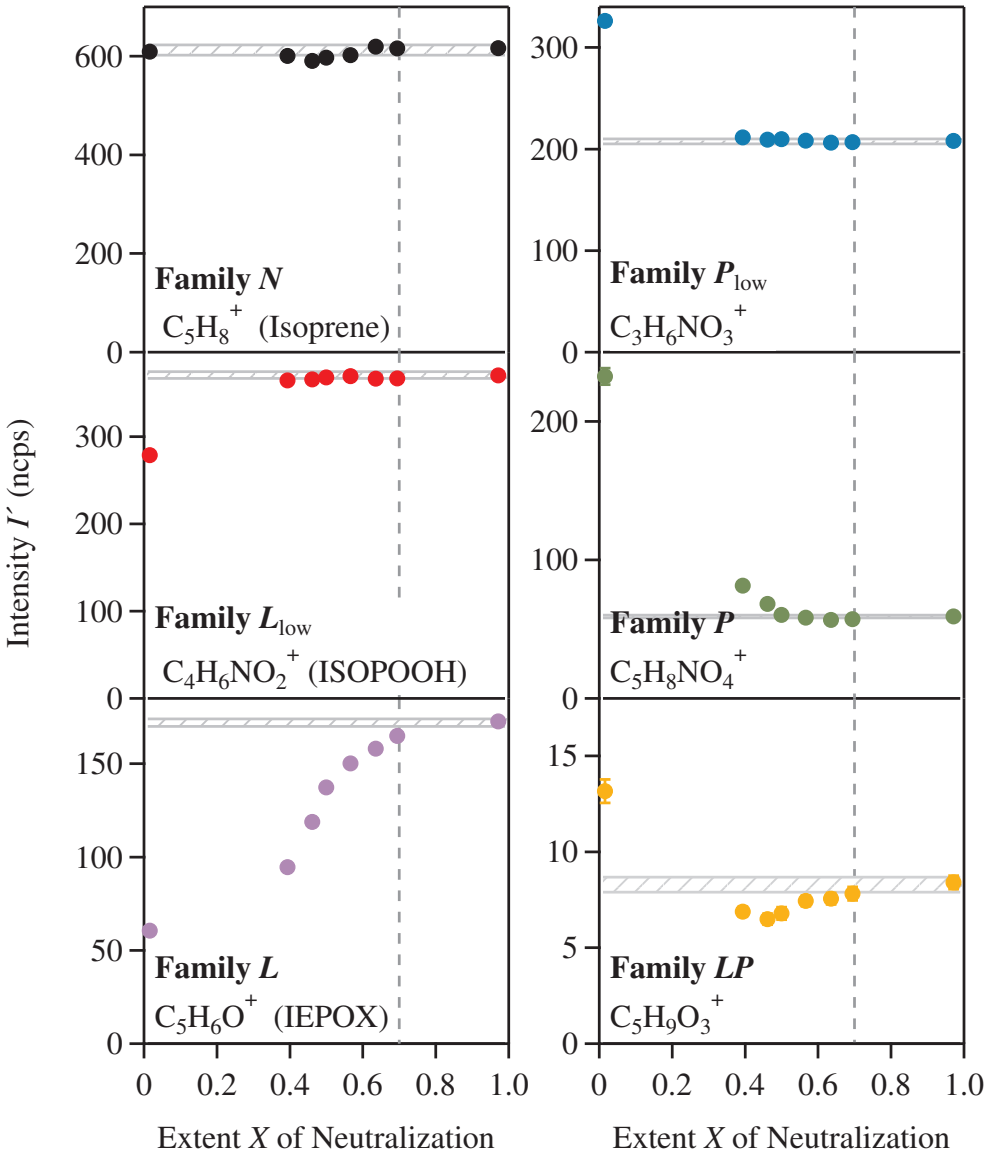
Intensity I′ (ncps)
Family N
C5H8+ (Isoprene)
Family Llow
C4H6NO2+ (ISOPOOH)
Family L
C5H6O+ (IEPOX)
Family Plow
C3H6NO3+
Family P
C5H8NO4+
Family LP
C5H9O3+
Extent X of Neutralization
Extent X of Neutralization

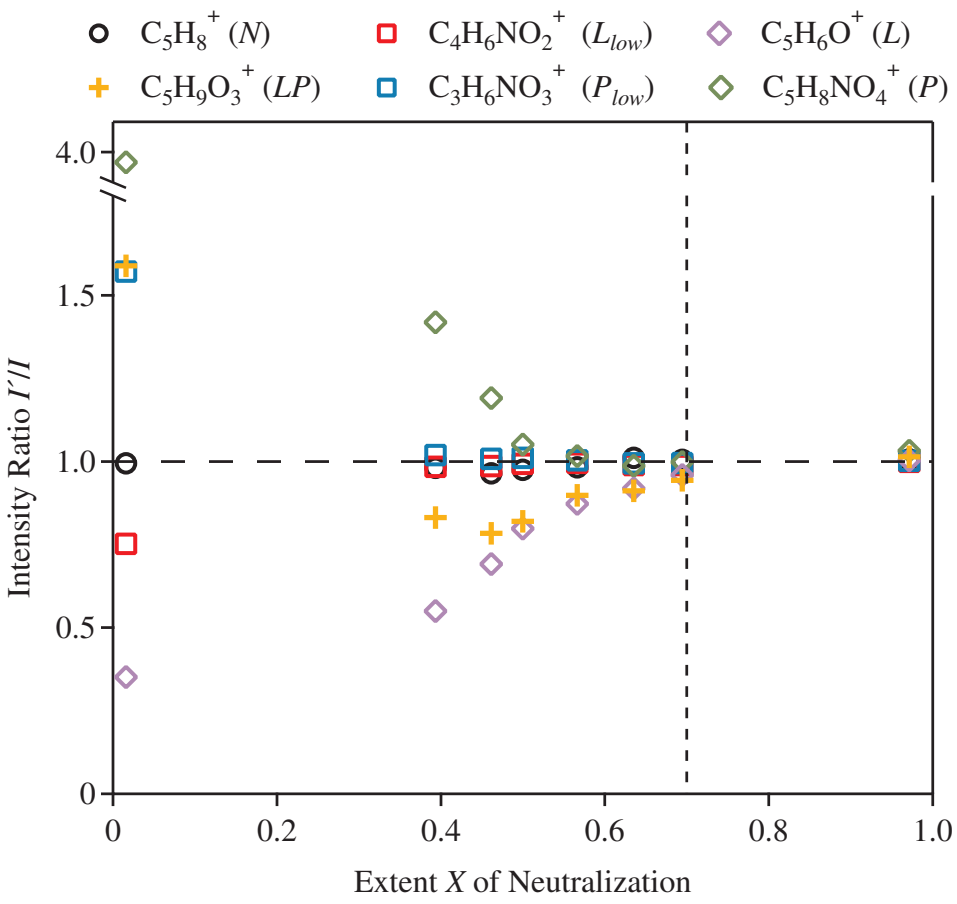
C5H8+ (N)
C4H6NO2+ (Llow)
C5H6O+ (L)
C5H9O3+ (LP)
C3H6NO3+ (Plow)
C5H8NO4+ (P)
4.0
1.5
1.0
0.5
0
Intensity Ratio I′/I
0
0.2
0.4
0.6
0.8
1.0
Extent X of Neutralization

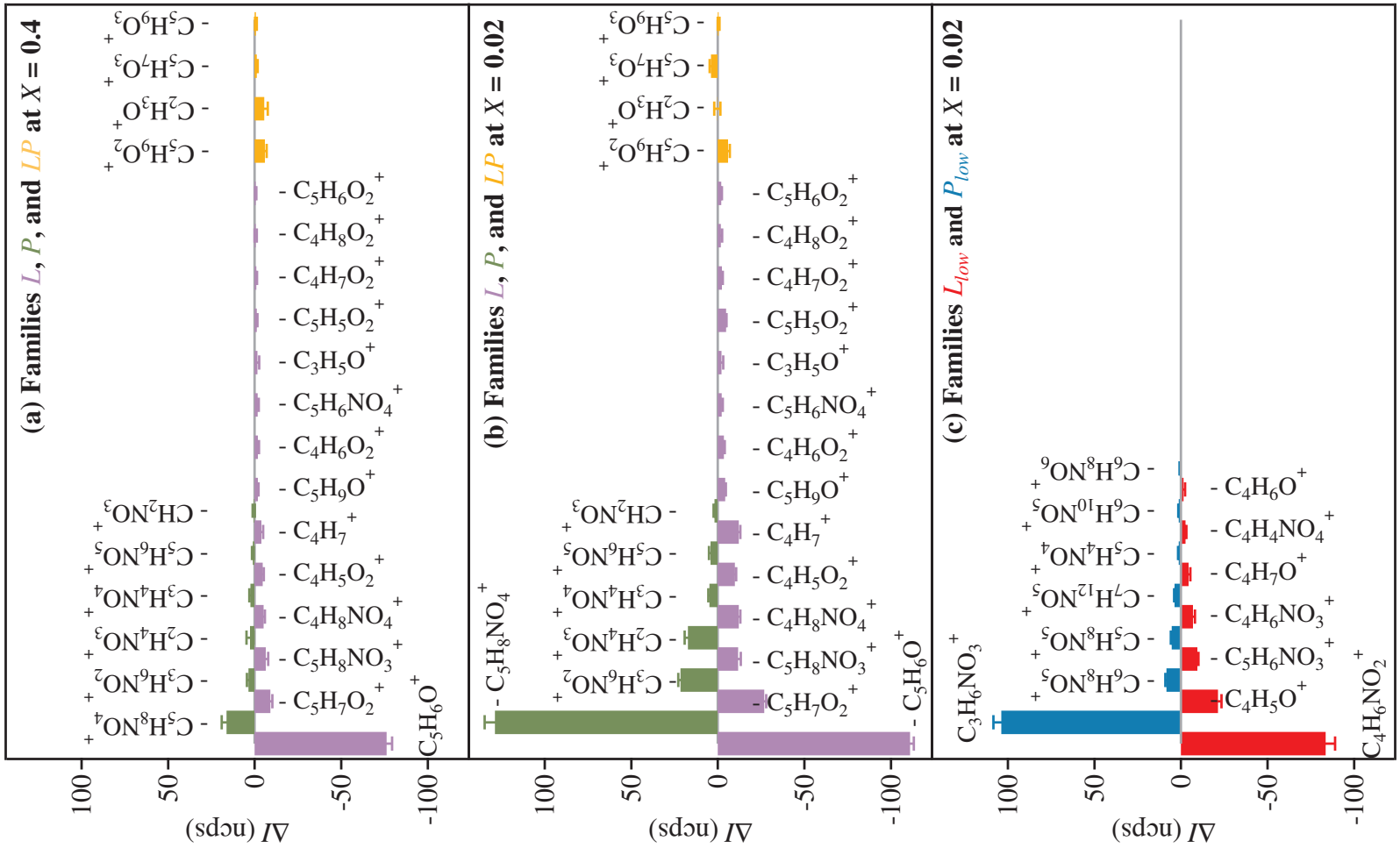
(a) Families L, P, and LP at X = 0.4
(b) Families L, P, and LP at X = 0.02
(c) Families L_low and P_low at X = 0.02
ΔI (ncps)
100
50
0
-50
-100
C5H6O+
C5H7O2+
C5H8NO3+
C4H8NO4+
C3H4NO4+
C2H4NO3+
C3H6NO2+
C5H8NO4+
CH2NO3+
C5H6NO5+
C4H5O2+
C4H7+
C5H9O+
C4H6O2+
C5H6NO4+
C3H5O+
C5H5O2+
C4H7O2+
C4H8O2+
C5H6O2+
C5H9O2+
C2H3O+
C5H7O3+
C5H9O3+
C5H6O+
C5H7O2+
C5H8NO3+
C4H8NO4+
C3H4NO4+
C2H4NO3+
C3H6NO2+
C5H8NO4+
CH2NO3+
C5H6NO5+
C4H5O2+
C4H7+
C5H9O+
C4H6O2+
C5H6NO4+
C3H5O+
C5H5O2+
C4H7O2+
C4H8O2+
C5H6O2+
C5H9O2+
C2H3O+
C5H7O3+
C5H9O3+
C4H6NO2+
C4H5O+
C5H6NO3+
C4H6NO3+
C4H7O+
C5H4NO4+
C4H4NO4+
C4H6O+
C6H8NO6+
C6H10NO5+
C7H12NO5+
C5H8NO5+
C6H8NO5+
C3H6NO3+